







# Double-core ionization photoelectron spectroscopy of C<sub>6</sub>H<sub>6</sub>: Breakdown of the “intuitive” *ortho-meta-para* binding energy ordering of K<sup>-1</sup>K<sup>-1</sup> states

Cite as: J. Chem. Phys. **151**, 214303 (2019); <https://doi.org/10.1063/1.5128614>

Submitted: 23 September 2019 . Accepted: 03 November 2019 . Published Online: 02 December 2019

S. Carniato, P. Selles, A. Ferté, N. Berrah, A. H. Wuosmaa, M. Nakano,  Y. Hikosaka,  K. Ito, M. Žitnik,  K. Bučar, L. Andric,  J. Palaudoux,  F. Penent,  P. Lablanquie, et al.



View Online



Export Citation



CrossMark

## ARTICLES YOU MAY BE INTERESTED IN

Excited states via coupled cluster theory without equation-of-motion methods: Seeking higher roots with application to doubly excited states and double core hole states

The Journal of Chemical Physics **151**, 214103 (2019); <https://doi.org/10.1063/1.5128795>

Vacuum ultraviolet photodissociation dynamics of CO<sub>2</sub> near 133 nm: The spin-forbidden O(<sup>3</sup>P<sub>j=2,1,0</sub>) + CO(X<sup>1</sup>Σ<sup>+</sup>) channel

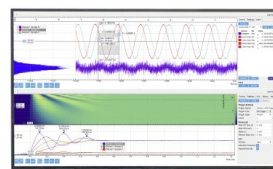
The Journal of Chemical Physics **151**, 214306 (2019); <https://doi.org/10.1063/1.5129764>

Multireference configuration interaction and perturbation theory without reduced density matrices

The Journal of Chemical Physics **151**, 211102 (2019); <https://doi.org/10.1063/1.5128115>

Challenge us.

What are your needs for periodic signal detection?



Zurich  
Instruments

# Double-core ionization photoelectron spectroscopy of $C_6H_6$ : Breakdown of the “intuitive” *ortho-meta-para* binding energy ordering of $K^{-1}K^{-1}$ states

Cite as: J. Chem. Phys. 151, 214303 (2019); doi: 10.1063/1.5128614

Submitted: 23 September 2019 • Accepted: 3 November 2019 •

Published Online: 2 December 2019



View Online



Export Citation



CrossMark

S. Carniato,<sup>1,a)</sup> P. Selles,<sup>1</sup> A. Ferté,<sup>1</sup> N. Berrah,<sup>2</sup> A. H. Wuosmaa,<sup>2</sup> M. Nakano,<sup>3</sup> Y. Hikosaka,<sup>4</sup> K. Ito,<sup>3,5</sup> M. Žitnik,<sup>6</sup> K. Bučar,<sup>6</sup> L. Andric,<sup>1</sup> J. Palaudoux,<sup>1</sup> F. Penent,<sup>1</sup> and P. Lablanquie<sup>1,a)</sup>

## AFFILIATIONS

<sup>1</sup>Laboratoire de Chimie Physique-Matière et Rayonnement (UMP 7614), Sorbonne Université, CNRS, 4 Place Jussieu, 75252 Paris Cedex 05, France

<sup>2</sup>Department of Physics, University of Connecticut, Storrs, Connecticut 06269, USA

<sup>3</sup>Photon Factory, Institute of Materials Structure Science, Tsukuba 305-0801, Japan

<sup>4</sup>Institute of Liberal Arts and Sciences, University of Toyama, Toyama 930-0194, Japan

<sup>5</sup>Synchrotron SOLEIL, l'Orme des Merisiers, Saint-Aubin, Boîte Postale 48, 91192 Gif-sur-Yvette Cedex, France

<sup>6</sup>Jozef Stefan Institute, Jamova Cesta 39, SI-1001 Ljubljana, Slovenija

<sup>a)</sup>Authors to whom correspondence should be addressed: [stephane.carniato@upmc.fr](mailto:stephane.carniato@upmc.fr) and [pascal.lablanquie@upmc.fr](mailto:pascal.lablanquie@upmc.fr)

## ABSTRACT

Single-site Double-Core Hole (ss-DCH or  $K^{-2}$ ) and two-site Double-Core Hole (ts-DCH or  $K^{-1}K^{-1}$ ) photoelectron spectra including satellite lines were experimentally recorded for the aromatic  $C_6H_6$  molecule using the synchrotron radiation and multielectron coincidence technique. Density functional theory and post-Hartree-Fock simulations providing binding energies and relative intensities allow us to clearly assign the main  $K^{-2}$  line and its satellites.  $K^{-1}K^{-1}$  states' positions and assignments are further identified using a core-equivalent model. We predict that, contrary to what has been observed in the  $C_2H_{2n}$  series of molecules, the  $K^{-1}K^{-1}$  energy-level ordering in  $C_6H_6$  does not reflect the core-hole distances between the two holes.

Published under license by AIP Publishing. <https://doi.org/10.1063/1.5128614>

## INTRODUCTION

A significant early application of spectroscopy in the X-ray domain was ESCA, electron spectroscopy for chemical analysis. In the X-ray spectral region, measurable chemical shifts are observed for core electron binding energies (BEs) of a given atom in different chemical environments.<sup>1–3</sup> The ESCA technique was then largely applied to the study of free molecules, molecules bonded on surfaces, and molecules in condensed and liquid phases.<sup>4–9</sup> Particularly, single core hole (SCH) states were investigated in the highly symmetric benzene molecule which is the prototypical system for many

aromatic molecules and building blocks in polymers and, more generally, for  $\pi$  electron systems. Photoabsorption near edge X-ray absorption fine structure (NEXAFS) spectra and photoelectron spectra in the X-ray domain (XPS) were measured and simulated for benzene in the gas-phase,<sup>10–15</sup> in adsorbed molecules<sup>16,17</sup> (an exhaustive list of references can be found therein), and in the condensed phase.<sup>18</sup>

However, the ESCA technique suffers from some limitations. Cederbaum and co-workers<sup>19</sup> demonstrated in 1986 that the spectroscopy of double-core holes (DCHs) would be more informative and sensitive than that of single-core holes: they predicted enhanced

chemical shifts for DCH states. Moreover, they anticipated that the bonding properties would be much more sensitive if the two core holes were created on two different atomic sites (ts-DCH) than on a single site (ss-DCH). Experimental confirmation of this pioneering prediction required 20 years after it was made, thanks to two experimental advances that developed independently and simultaneously:

On the one hand was the advent of intense X-ray Free-electron Laser (X-FEL) sources in the Angstrom wavelength. The first observation of molecular ss-DCH states with XFEL<sup>20</sup> was done at the Linac Coherent Light Source (LCLS) at SLAC in Stanford (CA, US) in 2009.<sup>21</sup> This technique was named “X-ray two-photon photoelectron spectroscopy” (XTPPS) because two photons were absorbed, each ejecting one photoelectron.<sup>22,23</sup>

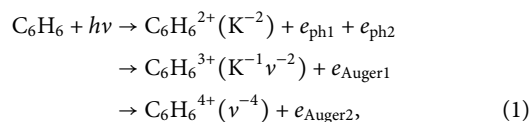
On the other hand was the introduction of efficient coincidence detection techniques based on the use of a magnetic bottle<sup>24</sup> for experiments done on the latest generation synchrotron sources. The first successful observation of ss-DCHs was performed in 2009 at the Photon Factory (Japan) on N<sub>2</sub> molecules,<sup>25</sup> followed by that of DCHs in O-containing molecules in February 2010 at SOLEIL (France).<sup>25</sup> This was followed very rapidly by the DCH experiments in CH<sub>4</sub> and NH<sub>3</sub> molecules in April 2010 at BESSY (Germany).<sup>26</sup> These DCHs arise from single-photon absorption, ejecting two electrons, due to electron correlations.<sup>25,26</sup>

Improved data processing for X-FEL-based experiments and improved statistics for synchrotron-based studies allowed the observation of ts-DCH states in small molecules such as N<sub>2</sub>, CO, C<sub>2</sub>H<sub>2n</sub>, NH<sub>3</sub>, and CH<sub>4</sub>.<sup>27</sup> On the theoretical side, DCH molecular states were investigated, mostly using the complete active space self-consistent field (CASSCF) method or density functional theory (DFT).<sup>28–32</sup> DCH satellites resulting from the simultaneous excitation of valence electrons upon core double ionization were observed<sup>25,33,34</sup> and found to be more intense than SCH satellites, relative to their main line. DCH satellite spectra of C<sub>2</sub>H<sub>2</sub>,<sup>33</sup> as well as N<sub>2</sub> and CO<sup>35</sup> molecules, were simulated using a generalization of the sudden approximation initially developed for single ionization.<sup>36,37</sup> Because the intensities of the transitions leading to multiple continuum are very difficult to handle, calculations of photoelectron spectra after multiple core ionization remain scarce. Apart from the previous calculations of the K<sup>-2</sup> satellite spectra cited above, to our knowledge, only one calculation based on a kinetic model was published; it concerns double-core photoionization of the organic *para*-aminophenol molecule by XFEL irradiation.<sup>22</sup>

Cederbaum *et al.* chose the benzene molecule<sup>38</sup> as a textbook case to illustrate the properties of ts-DCH states. The benzene molecule offers the opportunity to check three distinct groups of ts-DCH states: the two vacancies may be located in *ortho*-, *meta*-, or *para*-positions. In the present work, we present an experimental and computational study of DCH spectroscopy in benzene including satellite lines. After a description of the experimental setup and computational methods, the ss-DCH (or K<sup>-2</sup>) and ts-DCH (or K<sup>-1</sup>K<sup>-1</sup>) spectra are discussed. The three possible ts-DCH configurations are also predicted theoretically and discussed using a core-equivalent model. The satellite lines associated with the ss-DCH states are calculated using a post-Hartree-Fock (HF) configuration interaction (CI/SD) method. Detailed assignments of the peaks are proposed.

## EXPERIMENTAL DETAILS

The experiments were performed at the undulator beam line SEXTANTS<sup>39</sup> of the synchrotron facility SOLEIL in Saint-Aubin (France). The experimental setup HERMES is a magnetic bottle time-of-flight spectrometer of the type developed by Eland *et al.*<sup>24</sup> and is used under the single bunch operation mode of the synchrotron. Details can be found in Refs. 40 and 41 and the references therein. For the present experiment, performance was improved by reducing the dead time between the detection of two successive electrons. This was reduced to 2.5 ns, thanks to the use of the latest version of the time to digital analyzer (“TDCv4”) coupled with a fast leading edge discriminator, both developed at the LUMAT laboratory in Orsay, France. This dead time is an important characteristic for the measurement of double core hole processes because the shorter it is, the better one can separate electrons arriving successively at the detector. C<sub>6</sub>H<sub>6</sub><sup>2+</sup> double core holes decay dominantly within typically a few femtoseconds, by successive emission of two Auger electrons, following the reactions:



where  $e_{\text{phi}}$  are the emitted photoelectrons and  $\nu$  is a valence shell.

Figure 1 displays the spectrum of Auger electrons emitted in the decay of the C<sub>6</sub>H<sub>6</sub><sup>2+</sup> K<sup>-2</sup> ground state. In a similar way as for the C<sub>2</sub>H<sub>2n</sub> series of molecules,<sup>34,42</sup> two groups of Auger lines appear: above ~265 eV are the first emitted hypersatellite Auger electrons  $e_{\text{Auger}1}$ , while below 265 eV are the following Auger electrons  $e_{\text{Auger}2}$  emitted in the second step of the Auger decay. The K<sup>-2</sup> DCHs are

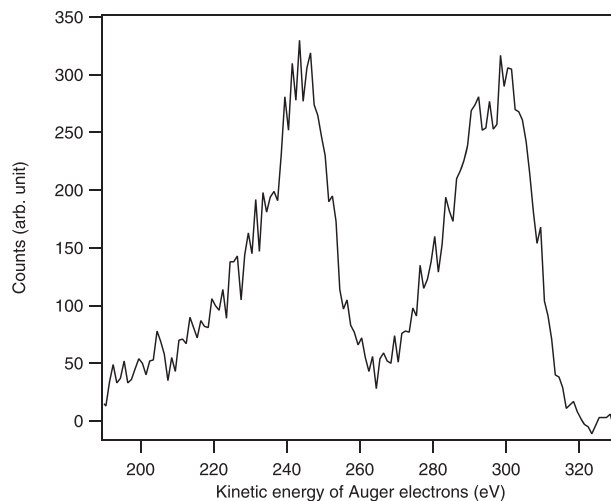


**FIG. 1.** Auger electrons emitted in the decay of the C<sub>6</sub>H<sub>6</sub><sup>2+</sup> K<sup>-2</sup> ground state. The spectrum was obtained by analyzing 4-electron coincidence events where two electrons are the photoelectrons emitted upon K<sup>-2</sup> ground state formation [Eq. (1)]. The higher energy band in the figure corresponds to the first Auger electron emitted in the cascade decay, while the lower one corresponds to the second one (see text for details).

identified by searching the data for events where 4 electrons are detected in coincidence, two of them being in the expected energy ranges for these Auger electrons, namely, [265–320 eV] and [190–265 eV]. The decay of  $K^{-1}K^{-1}$  two-site DCHs, on the contrary, releases two Auger electrons, each with energies between 190 and 265 eV. A long detector dead time ( $\sim 10$  ns) prevents the separation of these two Auger electrons and, in previous experiments,<sup>33,34</sup>  $K^{-1}K^{-1}$  DCHs could only be extracted from 3-electron coincidence events. The short 2.5 ns dead time that is achieved here corresponds to a blind zone in an energy of only  $\sim 5$  eV for 240 eV electrons. This improvement allowed us to search for  $K^{-1}K^{-1}$  DCHs in 4-electron coincidence events, two of these electrons being in the 190–265 eV energy range expected for the Auger electrons, thus reducing the experimental background.

The other points which were carefully checked were the photon energy and the electron kinetic energy calibrations. Figure 2 shows the  $K^{-2}$  ss-DCH spectrum (black dotted lines with error bars). The position of the double core ionization potential (DIP) was measured at  $647.8 \pm 1$  eV. The  $\pm 1$  eV error bar reflects the systematic uncertainty from the photon-energy and electron-kinetic energy scale. To reduce possible errors and possible drift of the photon energy, measurements in benzene were done immediately after measuring the  $C_2H_4$   $K^{-2}$  ss-DCH spectrum, under the same experimental conditions without changing the photon energy. The two spectra are compared in Fig. 2. Consequently, the relative DIP of the two molecules is measured with a reduced uncertainty of  $\pm 0.2$  eV, yielding a benzene DIP of  $-2.6 \pm 0.2$  eV less than that of  $C_2H_4$ .<sup>34</sup> Thus, this experimental method leads to a better estimate of the chemical shifts than the absolute DIP. This method was used to compare the chemical shifts of the Siegbahn molecule (ethyl trifluoroacetate,  $CF_3COOCH_2CH_3$ ) to that of  $C_2H_4$ .<sup>43</sup>

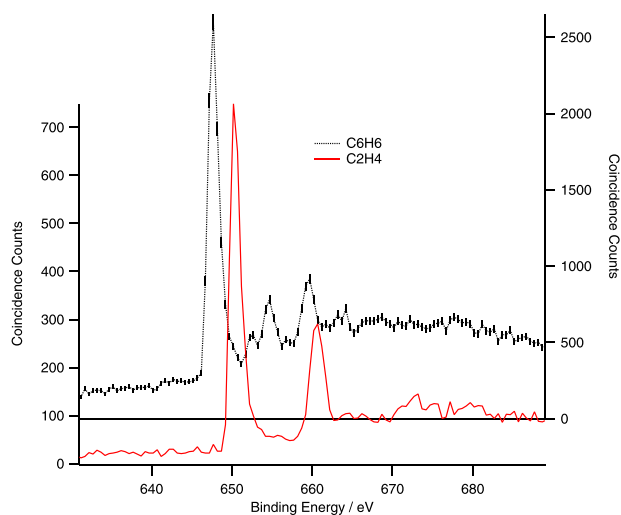


**FIG. 2.** Experimental  $K^{-2}$  double core hole spectrum of benzene compared to the  $K^{-2}$  double core hole spectrum of  $C_2H_4$  recorded in the same experimental conditions without changing the monochromator setting. This ensures that both spectra are recorded at exactly the same photon energy of 740 eV. In other words, the relative energy scales of the two spectra is free from the error bar originating from the photon energy scale calibration.

## THEORETICAL DETAILS

### Description of the initial and final states

Optimized geometries of the neutral  $C_6H_6$  ground state (see Fig. 3) were carried out in  $D_{6h}$  symmetry using the GAMESS (US)<sup>44</sup> package at a DFT level of theory, with the Becke three-parameter hybrid exchange<sup>45</sup> and the Lee-Yang-Parr gradient-corrected correlation functional (B3LYP).<sup>46</sup>

Calculations were done by adopting a localized description of the  $K^{-1}K^{-1}$  and  $K^{-2}$  double core-holes. This formulation proved to be necessary to estimate correctly the electronic relaxation and correlation effects.<sup>47,48</sup> The energy gap between the main line and the satellite lines is very sensitive to these effects.<sup>49</sup> Moreover, the delocalization of K electrons in the electronic ground state contributes an energy lowering of only a few tens of millielectronvolts for the K molecular orbital:<sup>38</sup> the population ratio between the four delocalized configurations  $(1a_{1g})^{-2}$ ,  $(1e_{1u})^{-2}$ ,  $(1e_{2g})^{-2}$ , and  $(1b_{1u})^{-2}$  with energy shifts 0/16/49/65 meV was estimated at 1/0.5/0.14/0.07, respectively. These values are out of reach of our experimental accuracy, justifying the use of a localized description. This choice of a localized description for the DCH lowers the  $D_{6h}$  molecular symmetry to the  $C_{2v}$  one. Within this scheme, initial neutral and final single-site double-core ionized states were characterized using a post-Hartree-Fock (HF) configuration interaction approach. This method relied on a unique set of orthogonal molecular orbitals constructed from RHF-SCF orthogonal orbitals optimized for the  $C$   $1s^{-2}$  state. For the surrounded C and H atoms, small basis sets of the 6-31G<sup>+</sup> type were used in which coefficients and orbital exponents were optimized from unrestricted Hartree-Fock (UHF) calculations combined with a simulated annealing procedure.<sup>50,51</sup> For the core-hole C atom, the 6-31G<sup>+</sup> set was augmented by (3s, 3p,

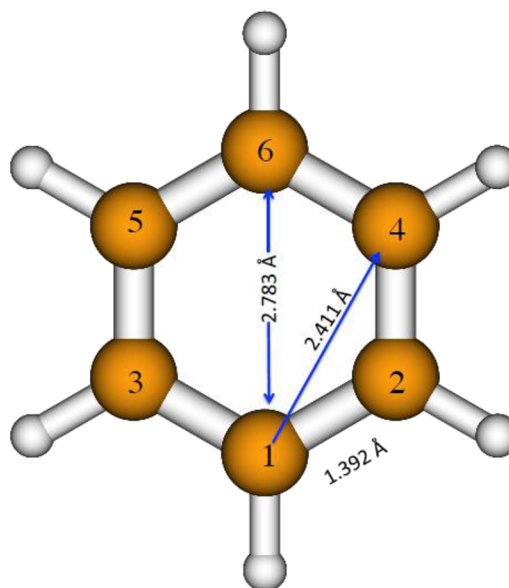


**FIG. 3.** Geometry and bond lengths in  $C_6H_6$ . With respect to carbon atom C1, the carbon atoms in *ortho*, *meta*, and *para* positions are, respectively, C2 and C3, C4 and C5, and C6.

3d) diffuse functions to simulate correctly the charge transfer.<sup>50</sup> As they were optimized for core-hole states, these small basis sets gave a balanced representation of all the core-hole sites and surrounding ligands. We have applied this method in previous studies.<sup>34,41,52</sup>

The total configuration interaction (CI) active space consists in the 15 doubly occupied valence orbitals (ignoring the six core orbitals) and the first 50 unoccupied virtual orbitals. Single, double, and triple valence (CI-SDT) excitations were taken into account in the description of the  $K^{-2}$  double core hole final states. The binding energies of the dominant satellite states with  $A_1$  symmetry were estimated. The neutral ground state was expanded in terms of single and double valence excitations. This large expansion was used in order to compensate for the choice of the molecular orbital set, which was not optimized for the neutral state. This choice of a unique reference set of molecular orbitals allowed a simpler evaluation of the overlap matrices taking place in the cross sections.

As for an accurate evaluation of binding energies of core-hole states,  $K^{-2}$  and  $K^{-1}K^{-1}$  single point energies were computed in the  $\Delta$ SCF (Delta Self Consistent Field) and  $\Delta$ KS/B3LYP/DK3 (Delta Kohn Sham with Douglas-Kroll relativistic effects at the third order) approaches. This latter density functional approach is well known to reproduce, in principle, most of the relaxation/correlation/relativistic effects upon core ionization or core excitation processes. These calculations were driven with an aug-cc-pV5Z basis set for carbon and hydrogen atoms.<sup>52</sup>

### Energy differential cross sections

An accurate calculation of single photon-double photoionization cross sections requires the description of the double continuum, which is beyond the purpose of this work. Here, we propose a model developed in the dipole approximation. The incident field is supposed to be entirely linearly polarized along the  $z$  axis in the laboratory frame. Only cross sections for the production of  $ss$ -DCH states and their satellites were estimated. In that case, our model considers that the two core electrons absorb a single photon instantaneously and escape simultaneously due to the attraction of the doubly charged molecular ion. After that, there is a relaxation of the remaining bound electrons in the presence of the double core hole. This model is an extension of the sudden approximation model initially developed for single photoionization.

The sixth order differential cross section, corresponding to the collection of two photoelectrons with asymptotic momenta  $\vec{k}_1$  and  $\vec{k}_2$ , is written in atomic units and in the length gauge as

$$\frac{d^6\sigma_f}{d\vec{k}_1 d\vec{k}_2} = 4\pi^2 \alpha\omega \left| \left\langle \vec{k}_1 \vec{k}_2 \psi_f(N-2) | D_z | \Psi_0(N) \right\rangle \right|^2 \delta(\omega - (E_f + \varepsilon); \Gamma_f), \quad (2)$$

where  $\Psi_0$  and  $\Psi_f$  represent the wave functions of the  $N$ -electron ground state and the  $(N-2)$ -electron DCH final state, respectively. Here,  $\omega$  is the energy of the incident photon,  $E_f$  is the binding energy of the final DCH state,  $\varepsilon$  is the total kinetic energy of the photoelectron pair,  $D_z$  is the component of the dipole operator along the polarization axis, and  $\delta(\omega; \Gamma_f)$  is the Lorentzian function

taking into account the lifetime of the final DCH state. No correlation is assumed between the bound and the free electrons in the final state. The line above the square modulus of the transition matrix element indicates an average on molecular orientations. In an interaction configuration description, the transition matrix element can be developed in the following way:

$$\left\langle \vec{k}_1 \vec{k}_2 \psi_f(N-2) | D_z | \Psi_0(N) \right\rangle = \sum_{ij} \left\langle \psi_f(N-2) | \hat{a}_i \hat{a}_j | \Psi_0(N) \right\rangle \times \left\langle \Phi_{\vec{k}_1, \vec{k}_2}^{\rightarrow, \rightarrow}(1, 2) | D_{z_1} + D_{z_2} | \phi_i(1) \phi_j(2) \right\rangle, \quad (3)$$

where the  $(i, j)$  summation runs over all the molecular spin-orbitals implied in the CI description of the initial wavefunction. The  $\Phi_{\vec{k}_1, \vec{k}_2}^{\rightarrow, \rightarrow}(1, 2)$  function describes the electron pair with the asymptotic momenta  $\vec{k}_1$  and  $\vec{k}_2$  in the continuum. The  $\hat{a}_i$  operators annihilate in the initial wave function the  $\Phi_i$  molecular spin-orbital. Because contributions of single and double core-excitations were not taken into account in the description of the initial state, and because a unique set of molecular orbitals was chosen for both the initial and the DCH states, the overlap matrix elements in the above equation are nonzero only if  $(i, j)$  refers to  $K$  orbitals.

Neglecting the interference between ionization pathways originating on different carbon atoms, the experimental yields corresponding to singly differential cross sections with respect to the photoelectron pair are given by the following expression:

$$\frac{d\sigma_f}{d\varepsilon} \propto I_f(\varepsilon) \left| \left\langle \Phi_f([K]^{-2}[\gamma]) | \hat{a}_{K\alpha} \hat{a}_{K\beta} | \Psi_0(N) \right\rangle \right|^2 \delta(\omega - (E_f + \varepsilon); \Gamma_f), \quad (4)$$

where  $\alpha$  and  $\beta$  refer to up and down electron spin states, respectively. The satellite lines correspond to  $[\gamma] = [v^{-1}V]$ . The final ionic state and the electron pair in the continuum are in a singlet spin state. The  $I_f(\varepsilon)$  integrals are obtained from integration of the molecular orientation averaged square modulus of the dipolar matrix element in the double momentum space as the experimental setup collects double photoelectron events in the whole space,

$$I_f(\varepsilon) = \int_0^\varepsilon d\varepsilon_2 \int d\vec{k}_1 \int d\vec{k}_2 \sqrt{(\varepsilon - \varepsilon_2)\varepsilon_2} \times \left| \left\langle \Phi_{\vec{k}_1, \vec{k}_2}^{\rightarrow, \rightarrow}(1, 2) | [D_{z_1} + D_{z_2}] | \phi_K(1) \phi_K(2) \right\rangle \right|^2. \quad (5)$$

In this expression,  $\Phi_{\vec{k}_1, \vec{k}_2}^{\rightarrow, \rightarrow}(1, 2)$  and  $\phi_K(i)$  are the spatial part of the singlet wavefunctions written in (3). The dependence on the excess energy of the dipolar intensities  $I_f(\varepsilon)$  should be negligible on an energy scale of about 10 eV around a central value of about 100 eV, so the theoretical model leads to a generalization of the expression written in Eq. (2) of Tashiro *et al.*<sup>35</sup>,

$$\frac{d\sigma_f}{d\varepsilon} \propto \left| \left\langle \Phi_f([K]^{-2}[\gamma]) | \hat{a}_{K\alpha} \hat{a}_{K\beta} | \Psi_0(N) \right\rangle \right|^2 \delta(\omega - (E_f + \varepsilon); \Gamma_f). \quad (6)$$

## RESULTS AND DISCUSSION

Figure 4 displays our experimental spectra for  $K^{-2}$  [Fig. 4(a)] and  $K^{-1}K^{-1}$  [Fig. 4(b)] DCH states. A multicoincidence data set was

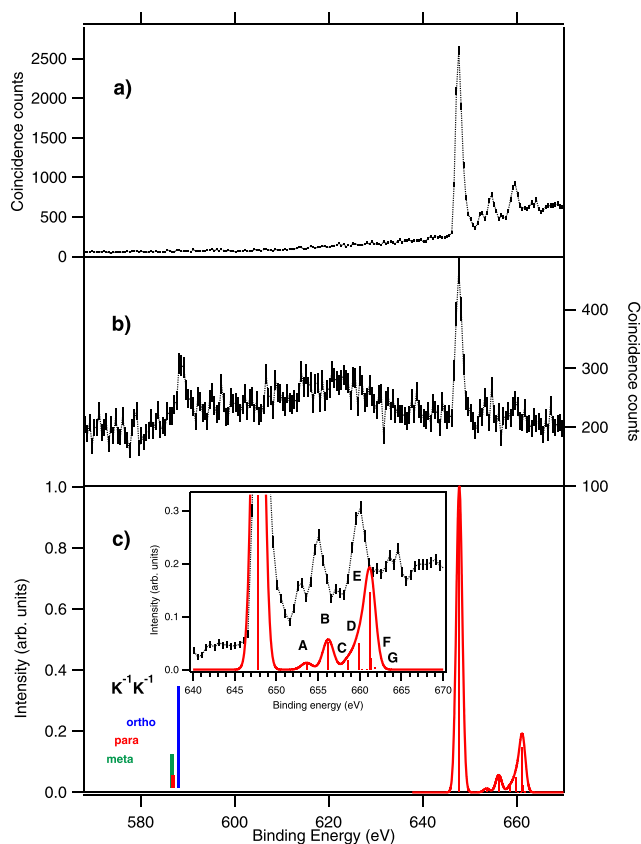


**FIG. 4.** Experimental  $K^{-2}$  (a) and  $K^{-1}K^{-1}$  (b) double core hole spectra of benzene recorded at a photon energy of 740 eV. (c) Theoretical  $K^{-2}$  double core hole spectrum. The inset displays an enlarged view of the satellite zone. The positions of the calculated  $K^{-1}K^{-1}$  double core hole states are indicated by vertical bars, whose height reflects their expected relative intensity, as populated in this 1-photon double core ionization process (see text for details).

accumulated for 20 h at a photon energy of 740 eV. As explained in the Experimental Details section, Fig. 4(a) was obtained from the 4-electron coincidence events where 2 electrons were found, respectively, in the energy ranges 265–320 eV and 190–265 eV, which are expected for the decay of the  $K^{-2}$  states (see Fig. 1). The  $K^{-2}$  ground state was observed at  $647.8 \pm 1$  eV, and a rich satellite structure appeared on the high binding energy side. As discussed above, the relative chemical shift compared to the  $C_2H_4$  molecule is measured at  $-2.6 \pm 0.2$  eV with smaller error bars.

To reveal ts-DCH states [Fig. 4(b)], we selected 4-electron coincidence events where 2 electrons are found in the same energy range [190–265 eV]. A contribution of the  $K^{-2}$  ground state remained due to the small possibility that the  $K^{-2}$  state decays by also emitting a first Auger electron in this [190–265 eV] energy range.  $K^{-1}K^{-1}$  DCH states clearly appeared at  $588.8 \pm 2$  eV. To reduce the background, we have excluded events with electron energies less than 10 eV.

### $K^{-1}K^{-1}$ process

Two-site DCH (ts-DCH) states have already been calculated in  $C_{60}$ , for which 23  $K^{-1}K^{-1}$  levels have been estimated.<sup>53</sup> In  $C_6H_6$ , only

three two-site thresholds are expected, corresponding to the removal of 1s electrons in two carbon atoms in *ortho* (1–2), *meta* (1–4), and *para* (1–6) positions (see Fig. 3). Only one peak is observed at  $588.8 \pm 2$  eV [see Fig. 4(b)] because our experimental resolution of about 2 eV is not sufficient to distinguish the three components which are predicted to be separated by at most 1 eV. In a previous paper, we demonstrated that the most probable process to create ts-DCHs is a knock-out mechanism in which a primary ionized K photoelectron ejects another K electron from a neighboring atom.<sup>53</sup> The probability for this process decreases quadratically with the distance between the two C atoms involved in the process so that we expect relative intensities of  $K^{-1}K^{-1}$  peaks to be 100/33/12 for C atoms in *ortho*, *meta*, and *para* positions, respectively (taking into account the number of possible C neighbors). This suggests that the observed experimental spectrum should be dominated by the ts-DCH path involving neighboring C atoms in *ortho* positions.

On the theoretical side, binding energies (BEs) of ts-DCH *ortho*, *meta*, and *para* states can be defined according to the Koopmans' approximation (frozen orbital approach) as

$$BE^{(0)}(a^{-1}b^{-1}) = -\varepsilon_a - \varepsilon_b + RE(a^{-1}b^{-1}), \quad (7)$$

where  $\varepsilon_a$  and  $\varepsilon_b$  are the Hartree Fock eigenvalues, chosen so that  $\varepsilon_a = \varepsilon_b = \bar{\varepsilon}_{1s} = -305.76$  eV, the average eigenvalue calculated from the six core orbitals. Here, the repulsion energy  $RE(a^{-1}b^{-1})$  between the two core holes must be taken into account. The repulsion energies are Coulomb energies calculated for two elementary positive charges located on each core-hole atom. The corresponding Koopman's binding energies  $BE^{(0)}$  (*ortho*),  $BE^{(0)}$  (*meta*), and  $BE^{(0)}$  (*para*) are collected in Table I. As expected, the ordering according to increasing binding energies is as follows:  $BE^{(0)}$  (*ortho*) >  $BE^{(0)}$  (*meta*) >  $BE^{(0)}$  (*para*). This intuitive order for the  $K^{-1}K^{-1}$  binding energies follows the two core-hole interatomic distance order, as previously observed in studies of the  $C_2H_{2n}$  ( $n = 1, 2, 3$ )<sup>23,54</sup> series. This order was also predicted by Cederbaum *et al.*,<sup>38</sup> using an ADC(2) method in a delocalized description.

To obtain more reliable estimates of the  $K^{-1}K^{-1}$  binding energies, we pushed our models beyond the Koopmans' approximation. Relaxation and correlation effects were accounted for by using  $\Delta$ SCF or  $\Delta$ KS procedures, which consist of a closed-shell SCF calculation for the neutral ground state and a restricted open-shell Hartree-Fock calculation (ROHF) for the ionized core states. The  $\Delta$ SCF and  $\Delta$ KS binding energies are reported in Table I. They are in mutual agreement and also agree well with the experimental value of  $588.2 \pm 2$  eV. The differences between the nonrelativistic  $\Delta$ KS and relativistic  $\Delta$ KS/DK3 binding energies amount to about 0.2 eV, corresponding to a relativistic correction of 0.1 eV for each 1s electron, in good agreement with the evaluation by Triguero *et al.*<sup>55</sup> The most noticeable result concerning  $\Delta$ SCF and  $\Delta$ KS values is the new binding energy ordering taking place when relaxation and correlation effects are taken into account.  $\Delta$ SCF and  $\Delta$ KS models both lead to the following classification:  $BE$  (*ortho*) >  $BE$  (*para*) >  $BE$  (*meta*) [(0, -0.88 eV, -1.58 eV) in the  $\Delta$ SCF model and (0.0, -0.99 eV, -1.23 eV) in the  $\Delta$ KS model]. Our models predict then an inversion of the regular order *meta/para* and do not confirm predictions by Cederbaum *et al.*<sup>38</sup>

TABLE I. Energies (in eV) associated with the *ortho*, *meta*, and *para*  $K^{-1}K^{-1}$  two-site DCH states. RE: repulsion energies between the two core holes. Binding energies are calculated by Koopman's theorem (KT) and  $\Delta$ SCF or  $\Delta$ KS methods. In the latter case, the two numbers in parentheses indicate the relativistic values obtained at Douglas-Kroll third order (DK3). RC2: generalized relaxation energies. BE(ADC2): binding energies obtained through an ADC2 model.

	$K^{-1}K^{-1}$			$K^{-1}$
	<i>Ortho</i>	<i>Meta</i>	<i>Para</i>	
RE	10.34	5.97	5.17	
Binding energy				
KT	621.96	617.59	616.79	305.76
$\Delta$ SCF	587.84	586.26	586.96	290.20
$\Delta$ KS (DK3)	587.78(96)	586.55(74)	586.79(98)	290.25 (35) (290.42) <sup>a</sup>
RC2				
$\Delta$ SCF	34.12	31.33	29.81	15.55
$\Delta$ KS	34.08	31.04	30.00	15.51
BE(ADC2)				
38	597.02	594.23	593.83	
Corrected	588.05	586.48	587.17	
$\Delta$ BE				
$\Delta$ SCF	7.44	5.86	6.56	
$\Delta$ KS	7.28 (7.26)	6.05 (6.04)	6.29 (6.28)	
(Z+1)	7.31	5.84	6.47	
IRC2				
$\Delta$ SCF	+2.90	+0.11	-1.39	
$\Delta$ KS	+3.06 (3.08)	-0.08 (-0.07)	-1.12 (-1.11)	
(Z+1)	+2.87	+0.13	-1.30	
IP( $b^{-1}/a^{-1}$ )				
$\Delta$ SCF	297.64	296.06	296.76	
$\Delta$ KS	297.43	295.91	296.44	
(Z+1)	297.67	296.04	296.67	

<sup>a</sup> $C_{1s}^{-1}$  experimental value.<sup>14</sup>  $\Delta$ BE: differential binding energies evaluated from Eq. (13). IRC2: interatomic generalized relaxation energies. IP( $b^{-1}/a^{-1}$ ): ionization potential for creating a CH  $b^{-1}$  1s core hole in the  $a^{-1}$  SCH state. In the (Z+1) core equivalent model, IP( $b^{-1}/a^{-1}$ ) is the ionization potential for creating a CH  $b^{-1}$  on a carbon atom in the pyridinium system  $[C_5NH_6]^+$ . That latter model is implemented in the  $\Delta$ SCF description at the DFT/B3LYP benzene molecular geometry.

This novel sequence *ortho/para/meta* predicted for the  $K^{-1}K^{-1}$  binding energies in benzene is similar to the one observed in the  $C_5H_5N$  molecular (pyridine) system, where it is well established<sup>51,56–58</sup> that the  $C_{1s}$  binding energies follow the same *ortho/para/meta* ordering. This ordering is already in place in the neutral ground state of pyridine as shown by the increasing *meta/para/ortho* Koopmans' eigenvalues<sup>51</sup> and remains unchanged even when additional relaxation/correlation effects are further considered. Koopmans' binding energies were evaluated for a series of conjugated and nonconjugated systems containing one terminal nitrogen atom presented in Table II. All Koopmans' binding energies display an *ortho/para/meta* order. This order is then an initial state effect for systems in which an atom of different electronegativity is present. To get deeper insight into the reasons for

this nonstandard *ortho/para/meta* ordering, we applied a very simple electrostatic model for molecules in Table II. The electrostatic model is that suggested by Aitken *et al.*<sup>59</sup> in which the HF binding energy of one atomic  $C_{1s}$  electron ( $-\epsilon_{at} = 308.0$  eV) is corrected by polarization effects,

$$BE(C_{1s}^{-1}) = -\epsilon_{at} + kq_i + \sum_{j=i}^N \frac{q_j}{r_{ij}}. \quad (8)$$

The  $q_j$  values are the partial valence electronic charges experienced by the atom  $j$  in the molecule. We took Löwdin values to modelize these charges. The constant  $k$  is fixed to the ionization potential in carbon, e.g., 11.37 eV, if  $q_i$  is positive and to the electronic affinity, e.g., 1.27 eV, if  $q_i$  is negative. The Coulomb last term mimics

**TABLE II.** Koopmans' binding energies evaluated for a series of chain and cyclic molecules containing one terminal nitrogen atom.

Butanamine NC <sub>4</sub> H <sub>11</sub>	NH <sub>2</sub>	CH <sub>2</sub>	CH <sub>2</sub>	CH <sub>2</sub>	CH <sub>3</sub>	
−ε <sub>1s</sub> (eV)		305.93	305.17	305.28	305.08	
Model						
q (Löwdin)		−0.018	−0.012	−0.013	0.121	
I <sub>1s</sub> (eV)		308.66	308.15	308.41	307.95	
Pentanamine NC <sub>5</sub> H <sub>13</sub>	NH <sub>2</sub>	CH <sub>2</sub>	CH <sub>2</sub>	CH <sub>2</sub>	CH <sub>2</sub>	CH <sub>3</sub>
−ε <sub>1s</sub> (eV)		305.92	305.16	305.21	305.23	305.04
Model						
q (Löwdin)		−0.017	−0.007	−0.002	−0.013	0.120
I <sub>1s</sub> (eV)		308.68	308.078	308.083	308.43	308.00
Pyridine NC <sub>5</sub> H <sub>5</sub>	N	( <i>Ortho</i> ) C <sub>1</sub> , C <sub>2</sub>	( <i>Meta</i> ) C <sub>3</sub> , C <sub>4</sub>	( <i>para</i> ) C <sub>5</sub>		
−ε <sub>1s</sub> (eV)		306.78	305.89	306.38		
Model						
q (Löwdin)		−0.032	−0.003	0.052		
I <sub>1s</sub> (eV)		308.50	308.27	308.32		
Pyridinium NC <sub>5</sub> H <sub>6</sub> <sup>+</sup>	N	( <i>Ortho</i> ) C <sub>1</sub> , C <sub>2</sub>	( <i>Meta</i> ) C <sub>3</sub> , C <sub>4</sub>	( <i>para</i> ) C <sub>5</sub>		
−ε <sub>1s</sub> (eV)		313.37	311.35	312.03		
Model						
q (Löwdin)		0.126	0.054	0.145		
I <sub>1s</sub> (eV)		316.27	315.46	315.08		

the effective potential produced by the neighboring atoms on the C<sub>i</sub> core-hole. Except for the pyridinium system, this simple model reproduces the *ortho/para/meta* order of the Koopmans' binding energies. It enlightens the role played by the surrounding atoms that participate in the polarization of the electronic cloud.

Generalized relaxation energies, RC2 (a<sup>−1</sup>b<sup>−1</sup>) contribute also to the understanding of the nonstandard *ortho/para/meta* ordering. Note that the R and C in RC2 (a<sup>−1</sup>b<sup>−1</sup>) stand, respectively, for relaxation and correlation energies. RC2 (a<sup>−1</sup>b<sup>−1</sup>) are defined as the difference between the binding energies BE<sup>(0)</sup> (a<sup>−1</sup>b<sup>−1</sup>)—see (7)—on one side and ΔSCF and ΔKS binding energies on the other,

$$\text{RC2}(a^{-1}b^{-1}) = \text{BE}^{(0)}(a^{-1}b^{-1}) - \text{BE}(a^{-1}b^{-1}). \quad (9)$$

Generalized relaxation energies are made of relaxation and correlation energies. They are collected in Table I. They are twice those we calculated for SCH states of benzene, making them reliable. For comparison, binding energies BE(a<sup>−1</sup>) and generalized relaxation energies RC(a<sup>−1</sup>) for SCH in benzene are also listed. Table I reveals that generalized relaxation energies deduced through ΔSCF or ΔKS methods are comparable. This unforeseen result indicates that differential electronic correlation effects ΔC taken into account in ΔKS calculations, but not considered in ΔSCF ones, are very small. This property derives from a subtle balance in which core-core, core-valence, and valence-valence correlation effects in the ground state

almost compensate new valence-valence correlation effects induced by the electronic relaxation in the DCH state.

The most important information concerns the ordering of generalized relaxation energies RC2(a<sup>−1</sup>b<sup>−1</sup>): these latter obey the following intuitive order: BE (*ortho*) > BE (*meta*) > BE (*para*). The collaborative electronic effects become more important when the core holes become closer. Moreover, relaxation and correlation effects are the key to understand and to erase the disagreement between Cederbaum's binding energy order and our binding energy order in benzene. Cederbaum *et al.* noted in their paper<sup>38</sup> that their ADC2 method was not expected to evaluate accurately electronic relaxation effects following double core hole vacancies. Indeed, their values for electronic relaxation were largely underestimated (about ~8 eV) compared to our values. Moreover, their differential *meta/para* relaxation energy was much smaller (0.4 eV) than our value (1.5 eV). We have thus corrected ADC2 binding energies of Ref. 38 according to the generalized relaxation energies we evaluated,

$$\text{BE}(\text{ADC2 corrected}) = \text{BE}(\text{ADC2}) + \text{RC2}(\text{ADC2}) - \text{RC2}(a^{-1}b^{-1}). \quad (10)$$

The ADC2 and the corrected ADC2 binding energies are shown in Table I. The BE(ADC2) and RC2(ADC2) values are extracted from Table II of Ref. 38. The resulting BE(ADC2corrected) follows now the order *ortho/para/meta*. The conclusion is then that the

unexpected order BE (*ortho*) > BE (*para*) > BE (*meta*) results from a subtle balance between the Coulombic repulsion acting between the two core-holes and the relaxation-correlation electronic effects, both of them being naturally ordered according to the *ortho/meta/para* sequence. Consequently, one will have to be very cautious in the interpretation of  $K^{-1}K^{-1}$  spectra and in the capabilities of a new spectroscopy<sup>22</sup> based on this effect since the energy ordering of states may possibly not follow a regular variation with interatomic distance.

In order to go even deeper in the analysis of these balance effects, a new quantity, the generalized interatomic relaxation energy, IRC2( $a^{-1}b^{-1}$ ), has been defined (by Cederbaum *et al.*<sup>38</sup> and Tashiro *et al.* 2010<sup>23</sup>) as

$$\text{IRC2}(a^{-1}b^{-1}) = \text{RC2}(a^{-1}b^{-1}) - [\text{RC}(a^{-1}) + \text{RC}(b^{-1})]. \quad (11)$$

This nonadditive quantity is an indicator of the environment of the core hole atoms. The IRC2 values give an estimation of the electronic density flow toward the two core hole sites relative to that in SCH states. Positive (negative) IRC2 values mean that creation of the second core hole enhances (decreases) the relaxation observed after creation of the first core-hole. All the pieces of information related to this ultimate analysis are collected in Table I. Generalized interatomic relaxation energies can be evaluated through the measurable differential binding energies  $\Delta\text{BE}$ ,

$$\text{IRC2}(a^{-1}b^{-1}) = \text{RE}(a^{-1}b^{-1}) - \Delta\text{BE}, \quad (12)$$

where

$$\Delta\text{BE} = \text{BE}(a^{-1}b^{-1}) - [\text{BE}(a^{-1}) + \text{BE}(b^{-1})]. \quad (13)$$

Our values collected in Table I indicate that a positive concerted relaxation happens in benzene when two core holes are created on two adjacent carbon atoms. This result is in agreement with the conclusions that can be found for polyatomic molecules in Refs. 23, 54, and 60. We find that the IRC decreases from positive to negative values as the hole-hole distance increases. Such a situation of a suppressed relaxation (negative values of IRC) for core hole states was first discussed by Tashiro *et al.*<sup>23</sup> Our (three) IRC values are however very different compared to the three positive values found for similar C–C distances in the 60 carbon fullerene ( $\text{C}_{60}$ ) compound.<sup>53</sup> This large apparent discrepancy is in fact due to a substantial overestimation of the theoretical  $\text{C}1s^{-1}$  core level binding energy value (291.1 eV, Takahashi *et al.*<sup>53</sup>) in  $\text{C}_{60}$  in comparison with the experimental measurements (290.10 eV, see the work of Liebsch *et al.*<sup>61</sup>). We re-examined the  $\text{C}_1^{-1}/\text{C}_2^{-1}$  ts-DCH of  $\text{C}_{60}$  after geometry optimization with a 6-31G\* basis set for carbons at the DFT/B3LYP level of theory. Using optimized 6-31G\* basis set for  $\text{C}1s^{-1}$ ,<sup>51</sup> we found 289.85 eV (and 290.15 eV with relativistic correction) in excellent agreement with experiments. Correction by  $-1.0$  eV of the corresponding calculated  $\text{C}1s^{-1}$  value in  $\text{C}_{60}$  provide similar values (3.0 eV/0.1 eV/0.9 eV) of IR as found in  $\text{C}_6\text{H}_6$ , indicating that the concerted relaxation energy is analogous in both benzene and fullerene aromatic compounds.

## $K^{-2}$ process

The ss-DCH ( $K^{-2}$ ) spectrum including the satellite lines is displayed in Fig. 4(a). It covers a large energy range ( $\approx 20$  eV) between

647 eV and 665 eV. The position of the double core ionization threshold (DIP) was estimated at  $647.8 \pm 1$  eV. This benzene DIP value is much lower than the values measured for the hydrocarbon series  $\text{C}_2\text{H}_n$  ( $n = 2/4/6$ ) but follows the same trend as observed for single K-shell ionization. The Hartree-Fock theoretical value of the  $K^{-2}$  ionization threshold (DIP) is found at 645.9 eV, e.g., 1.8 eV lower than the experimental value. The DFT/B3LYP theoretical value of the  $K^{-2}$  ionization threshold (DIP) is found at 645.2 eV and also suffers of a systematic underestimation ( $\approx -2.5$  eV) compared to the experimental value. Theoretical results already reported in previous studies (see Ref. 34) for hydrocarbons indicated such a systematic difference of 2.5 eV with respect to the experimental determinations. Assuming that this shift observed for hydrocarbons holds also for  $\text{C}_6\text{H}_6$ , its DIP is found in reasonable agreement with experimental measurements.

We evaluated generalized relaxation energies, defined for ss-DCH states according to the relation

$$\text{RC2}(a^{-2}) = -2\varepsilon_a + \text{RE}(a^{-2}) - \text{BE}(a^{-2}) = \text{BE}^{(0)}(a^{-2}) - \text{BE}(a^{-2}), \quad (14)$$

where  $\text{RE}(a^{-2})$  is the Coulomb repulsion for the two  $\text{C}(1s)$  holes localized on the same atom. It was estimated by the integral  $\text{RE}(a^{-2}) = \iint 1s^*(1)1s^*(2)\frac{1}{r_{12}}1s(1)1s(2)d\tau_1d\tau_2$ , at a Hartree-Fock level of theory using a very large aug-cc-pCV6Z basis set. It amounted to 95.5 eV, in excellent agreement with the 95.84 eV value extracted from the empirical formula derived by Cederbaum *et al.*,<sup>38</sup>

$$\text{RE}(1s^{-2}) = \left(\frac{2^{\frac{5}{2}}}{3\pi}\right)\left(1.037Z - 2^{-\frac{3}{2}}\right), \quad (15)$$

where  $Z$  is the atomic number of the atom with the two core holes.

From  $\Delta\text{SCF}$  Binding energy  $\text{BE}(a^{-2}) = 645.9$  eV, the DCH generalized relaxation energy  $\text{RC2}(a^{-2})$  was estimated from Eq. (14) to  $\approx 61$  eV, four times the relaxation energy for a SCH.

Differential relaxation energy defined as

$$\Delta\text{RC2}(a^{-2}) = \text{RC2}(a^{-2}) - 2\text{RC}(a^{-1}) \quad (16)$$

was evaluated at 30.01 and 30.82 eV in  $\Delta\text{SCF}$  and  $\Delta\text{KS}$  models, respectively. This differential relaxation energy is equivalent to the generalized interatomic relaxation energy defined in the case of ts-DCH. Experimental and theoretical ( $\Delta\text{SCF}$  and  $\Delta\text{KS}$ ) BEs for some ss-DCH nonaromatic and aromatic  $\pi$  bonds are collected in Table III. Even if absolute  $\Delta\text{SCF}$  and  $\Delta\text{KS}$  values are systematically underestimated compared to experimental ones, relative theoretical values and relative experimental values are in good agreement.

HF binding energies are nearly degenerate as  $\Delta\text{SCF}$  or  $\Delta\text{KS}$  values display a monotonic decay from acetylene ( $\text{C}_2\text{H}_2$ ) (triple bond) to ethylene ( $\text{C}_2\text{H}_4$ ) (double bond) and finally to benzene. This is mainly induced by different relaxation effects taking place in the final states. Relaxation energies  $\text{R2}(a^{-2})$  obtained as the difference between  $\Delta\text{SCF}$  and  $\text{BE}^{(0)}(a^{-2})$  values show larger effects for  $\text{C}_6\text{H}_6$  than for nonaromatic species. Generalized relaxation energies  $\text{RC2}(a^{-2})$  obtained as the difference between  $\Delta\text{KS}$  and  $\text{BE}^{(0)}(a^{-2})$

**TABLE III.** Binding energies  $BE(a^{-2})$  (in eV) for  $K^{-2}$  single-site DCH states in benzene and  $C_2H_{2n}$  molecules.  $\varepsilon_{1s}$  is the average C(1s) molecular orbital energy.  $RE(1s^{-2})$  is the Coulomb integral,  $RE(1s^{-2}) = 95.5$  eV.  $R2(a^{-2})$  are the relaxation energies and  $RC2(a^{-2})$  are the generalized relaxation energies including relaxation and differential correlation effects.

	$-\varepsilon_{1s}$	$-2\varepsilon_{1s} + RE(1s^{-2})$ (Koopmans)	$\Delta SCF$	R2	$\Delta KS$	RC2	$\Delta C2$	Expt.
$C_2H_2$	305.80	707.10	650.38	56.72	650.00	57.1	0.38	$652.5 \pm 0.5^{34}$
$C_2H_4$	305.54	706.58	648.17	58.41	647.95	58.63	0.23	$650.4 \pm 0.5^{34}$
$C_6H_6$	305.76	707.02	645.91	61.11	645.18	61.84	0.73	$647.8 \pm 1$ [this experiment]

values and including relaxation and differential correlation effects follow the same tendency. They revealed larger effects in the aromatic than in the linear molecules. Differential correlation energies defined as  $\Delta C2(a^{-2}) = C2(a^{-2}) - C(a)$ , where  $C(a)$  is the correlation energy in the initial neutral state, could be evaluated as the difference between  $RC2(a^{-2})$  and  $R2(a^{-2})$  values. They reveal a significant enhanced value for the benzene molecule. When comparing  $\Delta C2(a^{-1} b^{-1})$  (that can be read in Table I) and  $\Delta C2(a^{-2})$  values, we observe that differential correlation energies are larger in ss-DCH than in ts-DCH in benzene. Differential valence-valence correlation effects between the neutral and the double core hole states are mainly responsible for this situation. New valence-valence correlation effects induced by the larger electronic relaxation [ $4xR2(a^{-1})$ ] in the DCH states are much larger in the aromatic molecule than in the linear ones and much larger for ss-DCH than for ts-DCH states.

### $K^{-2}$ satellite structure

The  $K^{-2}$  experimental spectrum reveals in Fig. 4(a) weaker structures which correspond to  $K^{-2}$  satellite states where the double core hole ionization is accompanied by the simultaneous excitation of valence electrons.

$K^{-2}v(\text{valence})^{-n}v'(\text{virtual})^n$  ( $n = 1, 2, \dots$ ) satellite lines represent about 25% of the main  $K^{-2}$  line which is more than twice the value (10%) for satellite contribution in single core hole formation. It was already reported<sup>25</sup> that the relative intensities of satellites compared to the main peak are higher in DCH than those in SCH states.

The calculated spectrum is reported in Fig. 4(c). The model included single and up to triple excitations and was designed to cover the energy range of 640–660 eV. Although the model described in the Theoretical Details section was a rough model, most of the positions and intensities of the satellite lines agree reasonably well with experimental spectra.

In order to analyze in more detail the nature of the shake transitions, the molecular orbitals strongly involved in the shake-up excitations have been displayed in Fig. 5. Density plots of the outermost occupied CI wave-functions taking place in the building of lower-lying shake-up states are displayed. Since reconstruction of the CI orbital consists here in mixing orbitals of different symmetries ( $a_1$ ,  $b_{1,2}$ , or  $a_2$ ),  $C_{2v}$  symmetry is broken and densities are quite different from Hartree-Fock electronic densities of the low-lying unoccupied orbitals participating in the shake-up process. For  $C1s^{-2}$  in benzene (see Table IV), satellite lines correspond mainly to  $\pi\pi^*$  transition accompanying the ss-DCH ionization.

The first satellite region presents two peaks (labeled A and B) measured at 652.5 eV and 654.85 eV and calculated at  $BE = 653.63$  eV and  $BE = -656.20$  eV, respectively. As reported in Table IV, they are both mainly assigned to a linear combination of single  $1s^{-2}2b_1^1-3b_1^{1*}$  and  $1s^{-2}1a_2^1-2a_2^{1*}$  configurations involving the two outermost bonding orbitals ( $2b_1$ ,  $1a_2$ ) and the two lowest unoccupied antibonding orbitals ( $3b_1$ ,  $2a_2$ ) as well as minor additional double shake-up loss energies.

Another satellite state with very weak intensity is predicted at 658.65 eV (labeled C). This state is characterized by a combination of single  $1s^{-2}(1b_1^1 3b_1^{1*})/1s^{-2}(1a_2^1 2a_2^1)$  and mainly double  $2b_1^0 3b_1^{2*}/1a_1^0 3b_1^{2*}$  shake-up excitations. Due to poor statistics, the signature of this peak is not clearly identified in the experimental spectrum although a very weak shoulder is observed  $\sim 10$  eV at higher binding energy above the main peak.

The most intense satellite band is experimentally observed at 12 eV above the main peak around 660 eV. As shown in the present calculations, this region is marked by few satellite states. The calculated satellite states with substantial intensities were obtained at 659.92 eV, 661.2 eV, 661.4 eV, and 661.77 eV. In more detail, the peak (labeled D) with a 659.9 eV binding energy mainly corresponds to a linear combination of single  $1s^{-2}(2b_1^1 5b_1^1/2b_1^1 6b_1^1)$  and double shake-up  $1s^{-2}(1a_2^0 3b_1^2/2b_1^1 1a_2^1 3b_1^1 2a_2^1)$  transitions.

The satellite with larger intensity (labeled E) is mainly characterized by the single  $1s^{-2}1b_1^1 3b_1^{1*}$  transition involving the deeper

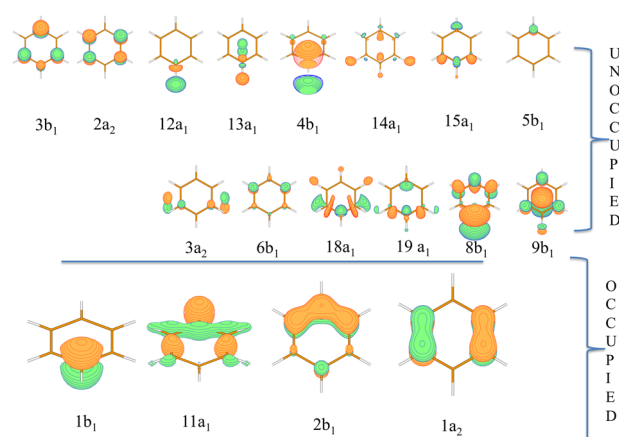


**FIG. 5.** Hartree-Fock electronic densities of the major outermost doubly occupied and low lying unoccupied orbitals participating to the  $C 1s^{-2}$  shake up process in  $C_6H_6$  in  $C_{2v}$  point group.

**TABLE IV.** Character and weights (in %) of contributed shake-up transitions in  $K^{-2}$  single-site DCH satellite states of  $C_6H_6$ . For each state (labeled A–G), more than 80% of the total configuration is indicated.

Configurations/labels	A	B	C	D	E	F	G
Relative energy (eV)	5.83	8.40	10.84	12.12	13.38	13.60	13.97
Relative intensity <sup>a</sup>	0.011	0.055	0.019	0.052	0.157	0.022	0.003
Single excitations							
$1b_1^1 3b_1^1$			10.5%	5%	57%	3%	
$11a_1^1 - 12a_1^1$				2%			
$11a_1^1 - 13a_1^1$							63%
$11a_1^1 - 15a_1^1$							6%
$11a_1^1 - 18a_1^1$							2.5%
$11a_1^1 - 19a_1^1$							2.5%
$2b_1^1 - 3b_1^1$	54%	25%		1%			
$2b_1^1 - 4b_1^1$				3%		8%	
$1a_2^1 - 2a_2^1$	18%	45%	18%		1.5%		
$1a_2^1 - 3a_2^1$				1%			
$2b_1^1 - 5b_1^1$			2.5%	9%			
$2b_1^1 - 6b_1^1$			3.5%	24.5%			
$1a_2^1 - 3a_2^1$					7.5%	63%	
$2b_1^1 - 8b_1^1$				3.5%			
$2b_1^1 - 9b_1^1$				2%			
Double excitations							
$2b_1^0 - 3b_1^2$	3%		14%	8%		2%	
$1a_2^0 - 2a_2^2$	1%	2%			1%	1.5%	
$2b_1^0 - 3b_1^1 6b_1^1$	1%						
$2b_1^1 1a_2^1 - 3b_1^1 2a_2^1$	4%	1%	1%	11%	2%	1%	
$1a_2^0 - 3b_1^1 6b_1^1$		1.5%	1%				
$1a_2^0 - 3b_1^2$	8%	6.5%	33%	13%	7.5%	2%	
$1b_1^1 2b_1^1 - 3b_1^2$					5%		
$2b_1^0 - 2a_2^2$		1.3%		2%			

<sup>a</sup>The reported intensities of satellites are calculated relative to the main peak intensity which is set to 1.

$1b_1$  mainly localized close to the double core ionized center and the  $3b_1^{1*}$  antibonding molecular orbital. The state is also the product of additional minor double shake transitions, as indicated in Table IV.

## CONCLUSION

In summary, we report here a detailed 4-electron coincidence experiment paired with a theoretical analysis of the ss-DCH  $K^{-2}$  and ts-DCH  $K^{-1}K^{-1}$  spectra in the  $C_6H_6$  molecular system. The ss-DCH  $K^{-2}$  spectrum is dominated by one main peak and two main shake-up lines clearly assigned as mainly out-of-plane  $\pi \rightarrow \pi^*$  ( $a_2 - a_2^*/b_1 - b_1^*$ ) secondary excitations, thanks to theory. The ts-DCH region was identified  $\approx 60$  eV below the ss-DCH threshold. The experimental spectrum shows only one peak. The low resolution cannot separate the three components which are expected.

Theory predicts that the binding energies BE of the three ts-DCH states are ordered in the following way: BE (*ortho*) > BE (*para*) > BE (*meta*). This is a surprising result as it does not reflect the core hole internuclear distance dependence (*ortho*) < (*meta*) < (*para*), contrary to what is observed in the  $C_2H_{2n}$  series.<sup>19,34</sup> The origin of this unusual property is traced back to a subtle balance between the Coulomb repulsion of the 2 core holes and the relaxation/correlation effects; it is clearly shown that the interatomic relaxation/correlation energy decreases from positive to negative values as the distance between the two core hole increases. The results based on the density functional theories agree with those based on the Hartree-Fock theory, illustrating the major role of the relaxation energy vs correlation energy.

Unfortunately, the present coincidence experiment cannot test our predictions, because of the weak cross section for 1-photon two-side core double ionization, and the subsequent weak signal.

It would, however, be interesting to use the FELs to form the three *ts*-DCH states in a 2-photon process using X-ray two-photon photoelectron spectroscopy (XTPPS). Here, contrary to what is expected in a 1-photon double ionization process, *ortho* and *meta* states should appear with similar intensities and twice that of the *para* state. It is expected that progress in the control of the XFEL properties and in the coincidence techniques will soon make possible such experiments. They would consist of observing the core photoionization of the carbon  $N^{\circ} b$  of a  $C_6H_6^+$  benzene ion where the carbon  $N^{\circ} a$  has already been ionized in its K-shell. Table I reports our predicted values for the resultant ionization potentials, which are deduced from our calculations presented above.

## ACKNOWLEDGMENTS

Preliminary experiments were done at the SOLEIL synchrotron (France) on the PLEIADES beamline with the approval of the Soleil Peer Review Committee (Project No. 20110211). The final experiments presented here were performed at SOLEIL at the SEXTANTS beamline with the approval of the Soleil Peer Review Committee (Project Nos. 20110875 and 20140129). We are grateful to A. Nicolaou and the SEXTANTS scientists and to C. Miron and the PLEIADES scientists for help during the measurements and to SOLEIL staff for stable operation of the storage ring during the experiments. K.I. acknowledges the support of the Labex Plas@Par, managed by the Agence Nationale de la Recherche, as part of the "Programme d'Investissements d'Avenir" under Reference No. ANR-11-IDEX-0004-02. N.B. acknowledges the support of the Chemical Sciences, Geosciences, and Biosciences Division, Office of Basic Energy Sciences, Office of Science, U.S. Department of Energy, Grant No. DE-SC0012376

## REFERENCES

- 1C. Nordling, E. Sokolowski, and K. Siegbahn, "Precision method for obtaining absolute values of atomic binding energies," *Phys. Rev.* **105**, 1676–1677 (1957).
- 2E. Sokolowski, C. Nordling, and K. Siegbahn, "Chemical shift effect in inner electronic levels of Cu due to oxidation," *Phys. Rev.* **110**, 776 (1958).
- 3K. Sieghnan, C. Nordling, A. Fahlmann, R. Nordberg, K. Hamerin, J. Hedman, G. Johansson, T. Bergmark, S. E. Karlsson, I. Lindgren, and B. Lindberg, *ESCA Electron Spectroscopy for Chemical Analysis: Atomic, Molecular and Solid State Structure Studied by Means of Electron Spectroscopy* (Almqvist and Wiksells, Sweden, 1967).
- 4U. Gelius, E. Basilier, S. Svensson, T. Bergmark, and K. Siegbahn, "A high resolution ESCA instrument with X-ray monochromator for gases and solids," *J. Electron Spectrosc. Relat. Phenom.* **2**, 405–434 (1973).
- 5G. van der Laan, C. Westra, C. Haas, and G. A. Sawatzky, "Satellite structure in photoelectron and Auger spectra of copper dihalides," *Phys. Rev. B* **23**, 4369–4380 (1981).
- 6N. S. McIntyre, S. Sunder, D. W. Shoosmith, and F. W. Stanchell, "Chemical information from XPS—Applications to the analysis of electrode surfaces," *J. Vac. Sci. Technol.* **18**, 714–721 (1981).
- 7H. Siegbahn and K. Siegbahn, "ESCA applied to liquids," *J. Electron Spectrosc. Relat. Phenom.* **2**, 319–325 (1973).
- 8H. Siegbahn, L. Asplund, P. Kelfve, K. Hamrin, L. Karlsson, and K. Siegbahn, "ESCA applied to liquids. II. Valence and core electron spectra of formamide," *J. Electron Spectrosc. Relat. Phenom.* **5**, 1059–1079 (1974).
- 9B. Lindberg, L. Asplund, H. Fellner-Feldegg, P. Kelfve, H. Siegbahn, and K. Siegbahn, "ESCA applied to liquids. ESCA spectra from molecular ions in solution," *Chem. Phys. Lett.* **39**, 8–10 (1976).
- 10J. A. Horsley, J. Stöhr, A. P. Hitchcock, D. C. Newbury, A. L. Johnson, and F. Sette, "Resonances in the K shell excitation spectra of benzene and pyridine: Gas phase, solid, and chemisorbed states," *J. Chem. Phys.* **83**, 6099–6107 (1985).
- 11A. P. Hitchcock, P. Fischer, A. Gedanken, and M. B. Robin, "Antibonding  $\sigma^*$  valence MOs in the inner-shell and outer-shell spectra of the fluorobenzenes," *J. Phys. Chem.* **91**, 531–540 (1987).
- 12M. N. Piancastelli, T. A. Ferrett, D. W. Lindle, L. J. Medhurst, P. A. Heimann, S. H. Liu, and D. A. Shirley, "Resonant processes above the carbon 1s ionization threshold in benzene and ethylene," *J. Chem. Phys.* **90**, 3004–3009 (1989).
- 13Y. Ma, F. Sette, G. Meigs, S. Modesti, and C. T. Chen, "Breaking of ground-state symmetry in core-excited ethylene and benzene," *Phys. Rev. Lett.* **63**, 2044–2047 (1989).
- 14E. E. Rennie, B. Kempgens, H. M. Köppe, U. Hergenhanh, J. Feldhaus, B. S. Itchkawitz, A. L. D. Kilcoyne, A. Kivimäki, K. Maier, M. N. Piancastelli, M. Polcik, A. Rüdell, and A. M. Bradshaw, "A comprehensive photoabsorption, photoionization, and shake-up excitation study of the C1s cross section of benzene," *J. Chem. Phys.* **113**, 7362–7375 (2000).
- 15R. Püttner, C. Kolczewski, M. Martins, A. S. Schlachter, G. Snell, M. Sant'Anna, J. Viehhaus, K. Hermann, and G. Kaindl, "The C1s NEXAFS spectrum of benzene below threshold: Rydberg or valence character of the unoccupied  $\sigma$ -type orbitals," *Chem. Phys. Lett.* **393**, 361–366 (2004).
- 16P. Zebisch, M. Stichler, P. Trischberger, M. Weinelt, and H.-P. Steinrück, "Tilted adsorption of benzene on Pt(110)  $1 \times 2$ ," *Surf. Sci.* **396**, 61–77 (1998).
- 17M. J. Kong, A. V. Teplyakov, J. G. Lyubovitsky, and S. F. Bent, "NEXAFS studies of adsorption of benzene on Si(100)- $2 \times 1$ ," *Surf. Sci.* **411**, 286–293 (1998).
- 18D. Menzel, G. Rucker, H.-P. Steinrück, D. Coulman, P. A. Heimann, W. Huber, P. Zebisch, and D. R. Lloyd, "Core excitation, decay, and fragmentation in solid benzene as studied by x-ray absorption, resonant Auger, and photon stimulated desorption," *J. Chem. Phys.* **96**, 1724–1734 (1992).
- 19L. S. Cederbaum, F. Tarantelli, A. Sgamellotti, and J. Schirmer, "On double vacancies in the core," *J. Chem. Phys.* **85**, 6513–6523 (1986).
- 20L. Fang, M. Hoerner, O. Gessner, F. Tarantelli, S. T. Pratt, O. Kornilov, C. Buth, M. Gühr, E. P. Kanter, C. Bostedt, J. D. Bozek, P. H. Bucksbaum, M. Chen, R. Coffee, J. Cryan, M. Glowina, E. Kuk, S. R. Leone, and N. Berrah, "Double core-hole production in  $N_2$ : Beating the Auger clock," *Phys. Rev. Lett.* **105**, 083005 (2010).
- 21P. Emma, R. Akre, J. Arthur, R. Bionta, C. Bostedt, J. Bozek, A. Brachmann, P. Bucksbaum, R. Coffee, F.-J. Decker, Y. Ding, D. Dowell, S. Edstrom, A. Fisher, J. Frisch, S. Gilevich, J. Hastings, G. Hays, Ph. Hering, Z. Huang, R. Iverson, H. Loos, M. Messerschmidt, A. Miahnahri, S. Moeller, H.-D. Nuhn, G. Pile, D. Ratner, J. Rzepiela, D. Schultz, T. Smith, P. Stefan, H. Tompkins, J. Turner, J. Welch, W. White, J. Wu, G. Yocky, and J. Galayda, "First lasing and operation of an Ångström-wavelength free-electron laser," *Nat. Photonics* **4**, 641–647 (2010).
- 22R. Santra, N. V. Kryzhevoi, and L. S. Cederbaum, "X-ray two-photon photoelectron spectroscopy: A theoretical study of inner-shell spectra of the organic *para*-aminophenol molecule," *Phys. Rev. Lett.* **103**, 013002 (2009).
- 23M. Tashiro, M. Ehara, H. Fukuzawa, K. Ueda, C. Buth, N. V. Kryzhevoi, and L. S. Cederbaum, "Molecular double core hole electron spectroscopy for chemical analysis," *J. Chem. Phys.* **132**, 184302 (2010).
- 24J. H. D. Eland, O. Vieuxmaire, T. Kinugawa, P. Lablanquie, R. I. Hall, and F. Penet, "Complete two-electron spectra in double photoionization: The rare gases Ar, Kr, and Xe," *Phys. Rev. Lett.* **90**, 053003 (2003).
- 25P. Lablanquie, F. Penet, J. Palaudoux, L. Andric, P. Selles, S. Carniato, K. Bučar, M. Žitnik, M. Huttula, J. H. D. Eland, E. Shigemasa, K. Soejima, Y. Hikosaka, I. H. Suzuki, M. Nakano, and K. Ito, "Properties of hollow molecules probed by single-photon double ionization," *Phys. Rev. Lett.* **106**, 063003 (2011).
- 26J. H. D. Eland, M. Tashiro, P. Linusson, M. Ehara, K. Ueda, and R. Feifel, "Double core hole creation and subsequent Auger decay in  $NH_3$  and  $CH_4$  molecules," *Phys. Rev. Lett.* **105**, 213005 (2010).

- <sup>27</sup>N. Berrah, L. Fang, B. Murphy, T. Osipov, K. Ueda, E. Kukk, R. Feifel, P. van der Meulen, P. Salen, H. T. Schmidt, R. D. Thomas, M. Larsson, R. Richter, K. C. Prince, J. D. Bozek, C. Bostedt, S.-i. Wada, M. N. Piancastelli, M. Tashiro, and M. Ehara, "Double-core-hole spectroscopy for chemical analysis with an intense X-ray femtosecond laser," *Proc. Natl. Acad. Sci. U. S. A.* **108**, 16912–16915 (2011).
- <sup>28</sup>M. Tashiro, K. Ueda, and M. Ehara, "Auger decay of molecular double core-hole state," *J. Chem. Phys.* **135**, 154307 (2011).
- <sup>29</sup>N. V. Kryzhevoi, R. Santra, and L. S. Cederbaum, "Inner-shell single and double ionization potentials of aminophenol isomers," *J. Chem. Phys.* **135**, 084302 (2011).
- <sup>30</sup>O. Takahashi, M. Tashiro, M. Ehara, K. Yamasaki, and K. Ueda, "Theoretical spectroscopy on  $K^{-2}$ ,  $K^{-1}L^{-1}$ , and  $L^{-2}$  double core hole states of  $\text{SiX}_4$  ( $X=\text{H, F, Cl, and CH}_3$ ) molecules," *Chem. Phys.* **384**, 28–35 (2011).
- <sup>31</sup>K. Ueda and O. Takahashi, "Extracting chemical information of free molecules from K-shell double core-hole spectroscopy," *J. Electron Spectrosc. Relat. Phenom.* **185**, 301–311 (2012).
- <sup>32</sup>T. D. Thomas, "Single and double core-hole ionization energies in molecules," *J. Phys. Chem. A* **116**, 3856–3865 (2012).
- <sup>33</sup>P. Lablanquie, T. P. Grozdanov, M. Žitnik, S. Carniato, P. Selles, L. Andric, J. Palaudoux, F. Penent, H. Iwayama, E. Shigemasa, Y. Hikosaka, K. Soejima, M. Nakano, I. H. Suzuki, and K. Ito, "Evidence of single-photon two-site core double ionization of  $\text{C}_2\text{H}_2$  molecules," *Phys. Rev. Lett.* **107**, 193004 (2011).
- <sup>34</sup>M. Nakano, F. Penent, M. Tashiro, T. P. Grozdanov, M. Žitnik, S. Carniato, P. Selles, L. Andric, P. Lablanquie, J. Palaudoux, E. Shigemasa, H. Iwayama, Y. Hikosaka, K. Soejima, I. H. Suzuki, N. Kouchi, and K. Ito, "Single photon  $K^{-2}$  and  $K^{-1}K^{-1}$  double core ionization in  $\text{C}_2\text{H}_{2n}$  ( $n=1-3$ ), CO, and  $\text{N}_2$  as a potential new tool for chemical analysis," *Phys. Rev. Lett.* **110**, 163001 (2013).
- <sup>35</sup>M. Tashiro, K. Ueda, and M. Ehara, "Double core-hole correlation satellite spectra of  $\text{N}_2$  and CO molecules," *Chem. Phys. Lett.* **521**, 45–51 (2012).
- <sup>36</sup>T. Åberg, *Phys. Rev.* **156**, 35–41 (1967).
- <sup>37</sup>R. Manne and T. Åberg, "Koopmans' theorem for inner-shell ionization," *Chem. Phys. Lett.* **7**, 282–284 (1970).
- <sup>38</sup>L. S. Cederbaum, F. Tarantelli, A. Sgamellotti, and J. Schirmer, "Double vacancies in the core of benzene," *J. Chem. Phys.* **86**, 2168–2175 (1987).
- <sup>39</sup>S. G. Chiuabäian, C. F. Hague, A. Avila, R. Delaunay, N. Jaouen, M. Sacchi, F. Polack, M. Thomasset, B. Lagarde, A. Nicolaou, S. Brignolo, C. Baumier, J. Lüning, and J.-M. Mariot, "Design and performance of AERHA, a high acceptance high resolution soft x-ray spectrometer," *Rev. Sci. Instrum.* **85**, 043108 (2014).
- <sup>40</sup>J. Palaudoux, S.-M. Huttula, M. Huttula, F. Penent, L. Andric, and P. Lablanquie, "Auger decay paths of mercury  $5p$  and  $4f$  vacancies revealed by multielectron spectroscopy," *Phys. Rev. A* **91**, 012513 (2015).
- <sup>41</sup>S. Carniato, P. Selles, L. Andric, J. Palaudoux, F. Penent, M. Žitnik, K. Bučar, M. Nakano, Y. Hikosaka, K. Ito, and P. Lablanquie, "Single photon simultaneous K-shell ionization and K-shell excitation. II. Specificities of hollow nitrogen molecular ions," *J. Chem. Phys.* **142**, 014308 (2015).
- <sup>42</sup>F. Penent, M. Nakano, M. Tashiro, T. P. Grozdanov, M. Žitnik, S. Carniato, P. Selles, L. Andric, P. Lablanquie, J. Palaudoux, E. Shigemasa, H. Iwayama, Y. Hikosaka, K. Soejima, I. H. Suzuki, N. Kouchi, and K. Ito, "Molecular single photon double K-shell ionization," *J. Electron Spectrosc. Relat. Phenom.* **196**, 38–42 (2014).
- <sup>43</sup>F. Penent, M. Nakano, M. Tashiro, T. P. Grozdanov, M. Žitnik, K. Bučar, S. Carniato, P. Selles, L. Andric, P. Lablanquie, J. Palaudoux, E. Shigemasa, H. Iwayama, Y. Hikosaka, K. Soejima, I. H. Suzuki, N. Berrah, A. H. Wuosmaa, T. Kaneyasu, and K. Ito, "Double core hole spectroscopy with synchrotron radiation," *J. Electron Spectrosc. Relat. Phenom.* **204**, 303–312 (2015).
- <sup>44</sup>M. W. Schmidt, K. K. Baldrige, J. A. Boatz, S. T. Elbert, M. S. Gordon, J. H. Jensen, S. Koseki, N. Matsunaga, K. A. Nguyen, S. Su, T. L. Windus, M. Dupuis, and J. A. Montgomery, "General atomic and molecular electronic structure system," *J. Comput. Chem.* **14**, 1347–1363 (1993).
- <sup>45</sup>A. D. Becke, "Density-functional thermochemistry. III. The role of exact exchange," *J. Chem. Phys.* **98**, 5648–5652 (1993).
- <sup>46</sup>C. Lee, W. Yang, and R. G. Parr, "Development of the Colle-Salvetti correlation-energy formula into a functional of the electron density," *Phys. Rev. B* **37**, 785–789 (1988).
- <sup>47</sup>P. S. Bagus and H. F. Schaefer, "Localized and delocalized  $1s$  hole states of the  $\text{O}_2^+$  molecular ion," *J. Chem. Phys.* **56**, 224–226 (1972).
- <sup>48</sup>R. Broer and W. C. Nieuwpoort, "Broken orbital-symmetry and the description of hole states in the tetrahedral  $[\text{CrO}_4]^-$  anion. I. Introductory considerations and calculations on oxygen  $1s$  hole states," *Chem. Phys.* **54**, 291–303 (1981).
- <sup>49</sup>M. Ehara, K. Kuramoto, H. Nakatsuji, M. Hoshino, T. Tanaka, M. Kitajima, H. Tanaka, A. De Faniis, Y. Tamenori, and K. Ueda, "C1s and O1s photoelectron satellite spectra of CO with symmetry-dependent vibrational excitations," *J. Chem. Phys.* **125**, 114304 (2006).
- <sup>50</sup>S. Carniato and P. Millié, "Accurate core electron binding energy calculations using small 6-31G and TZV core hole optimized basis sets," *J. Chem. Phys.* **116**, 3521–3532 (2002).
- <sup>51</sup>S. Carniato and Y. Luo, "Role of differential correlation energy in core ionization of pyrrole and pyridine," *J. Electron Spectrosc. Relat. Phenom.* **142**, 163–171 (2005).
- <sup>52</sup>S. Carniato, P. Selles, L. Andric, J. Palaudoux, F. Penent, M. Žitnik, K. Bučar, M. Nakano, Y. Hikosaka, K. Ito, and P. Lablanquie, "Single photon simultaneous K-shell ionization and K-shell excitation. I. Theoretical model applied to the interpretation of experimental results on  $\text{H}_2\text{O}$ ," *J. Chem. Phys.* **142**, 014307 (2015).
- <sup>53</sup>O. Takahashi and K. Ueda, "Molecular double core-hole electron spectroscopy for probing chemical bonds:  $\text{C}_{60}$  and chain molecules revisited," *Chem. Phys.* **440**, 64–68 (2014).
- <sup>54</sup>M. Tashiro, M. Ehara, and K. Ueda, "Double core-hole electron spectroscopy for open-shell molecules: Theoretical perspective," *Chem. Phys. Lett.* **496**, 217–222 (2010).
- <sup>55</sup>L. Triguero, O. Plashkevych, L. G. M. Pettersson, and H. Ågren, "Separate state vs. transition state Kohn-Sham calculations of X-ray photoelectron binding energies and chemical shifts," *J. Electron Spectrosc. Relat. Phenom.* **104**, 195–207 (1999).
- <sup>56</sup>St. Hövel, C. Kolczewski, M. Wühh, J. Albers, K. Weiss, V. Staemmler, and Ch. Wöll, "Pyridine adsorption on the polar  $\text{ZnO}(0001)$  surface: Zn termination versus O termination," *J. Chem. Phys.* **112**, 3909–3916 (2000).
- <sup>57</sup>C. Kolczewski, R. Püttner, O. Plashkevych, H. Ågren, V. Staemmler, M. Martins, G. Snell, A. S. Schlachter, M. Sant'Anna, G. Kaindl, and L. G. M. Pettersson, "Detailed study of pyridine at the C1s and N1s ionization thresholds: The influence of the vibrational fine structure," *J. Chem. Phys.* **115**, 6426–6437 (2001).
- <sup>58</sup>C. Hannay, D. Duflo, J.-P. Flament, and M.-J. Hubin-Franskin, "The core excitation of pyridine and pyridazine: An electron spectroscopy and *ab initio* study," *J. Chem. Phys.* **110**, 5600–5610 (1999).
- <sup>59</sup>E. J. Aitken, M. K. Bahl, K. D. Bomben, J. K. Gimzewski, G. S. Nolan, and T. D. Thomas, "Electron spectroscopic investigations of the influence of initial- and final-state effects on electronegativity," *J. Am. Chem. Soc.* **102**, 4873–4879 (1980).
- <sup>60</sup>O. Takahashi, M. Tashiro, M. Ehara, K. Yamasaki, and K. Ueda, "Theoretical molecular double-core-hole spectroscopy of nucleobases," *J. Phys. Chem. A* **115**, 12070–12082 (2011).
- <sup>61</sup>T. Liesch, O. Plotzke, F. Heiser, U. Hergenbahn, O. Hemmers, R. Wehlitz, J. Viehhaus, B. Langer, S. B. Whitfield, and U. Becker, "Angle-resolved photoelectron spectroscopy of  $\text{C}_{60}$ ," *Phys. Rev. A* **52**, 457–464 (1995).